DIAGONAL TENSION IN FIBRE-METAL LAMINATES

A. Jodoin[1], C. Poon[2], P.V. Straznicky[1], G. Shi[2], and L. Kok[3]
[1]Department of Mechanical and Aerospace Engineering
Carleton University, 1125 Colonel By Drive, Ottawa, Ontario, Canada K1S 5B6
[2]Structures, Materials and Propulsion Laboratory
Institute for Aerospace Research, National Research Council Canada
Ottawa, Ontario, Canada K1A 0R6
[3]Bombardier Aerospace, Structures Research & Development,
123 Garratt Blvd., MS N46-36, Downsview, Ontario, Canada, M3K 1Y5

Keywords: *diagonal tension, FML, GLARE, shear buckling*

Abstract

As part of a larger ongoing collaborative project between the National Research Council Canada (NRC), Bombardier Aerospace and Carleton University, various GLARE (GLAss REinforced aluminum) web materials were tested to determine their performance while in a state of diagonal tension. Of importance was the evaluating of the validity of the National Advisory Committee for Aeronautics (NACA) methodology developed for aluminum alloys, when applied to predicting the yielding and failure of GLARE-webs. Each test specimen is a 2.06 m x 0.79 m flat beam emulation of an aircraft stiffened thin skin. The diagonal tension effect is simulated in the test specimen by applying an in-plane shear load. Under increasing shear stress in the beam, the web material buckles elastically, then forms permanent buckles, and finally suffers a critical failure. The tests were conducted using the Institute for Aerospace Research's Multi-Actuator Test Platform, a new facility for testing large aircraft components and sub-assemblies. Varying thickness of GLARE 3, GLARE 4, and 2024-T3 aluminum were tested. The results have shown that the NACA-based methodology can be used to predict GLARE web stress/strain reactions up to its yield point. However, more detailed studies into the plastic buckling behavior of GLARE will have to be conducted to accurately predict critical failures.

1 Introduction

Fibre-metal laminates (FMLs) are increasingly being used in the design of secondary and tertiary aircraft structural components such as cargo bay floors, bulkheads, access hatches and wing flaps. However, the constant effort to make aircraft stronger and lighter has now led to studies to determine the feasibility of constructing primary aircraft structures using this new class of material. A priority of these studies is determining the potential applications of GLARE (GLAss REinforced aluminum): a laminate composed of alternating layers of thin aluminum sheets and unidirectional or cross-ply glass-fiber/epoxy (Fig. 1).

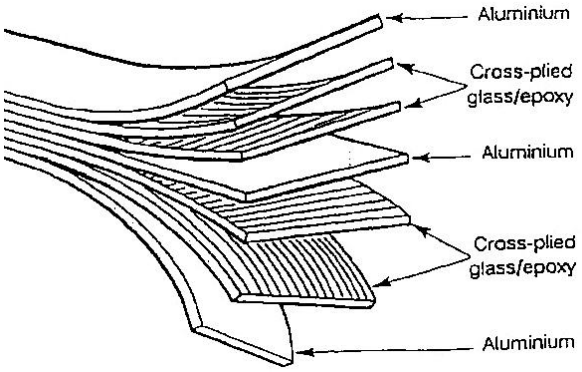

Fig. 1. Composition lay-up of GLARE 3 – 3/2 [1]

As part of a larger ongoing collaborative FML project between the NRC, Bombardier Aerospace and Carleton University, efforts are being made to understand the behaviour of GLARE in aircraft structures.

In general, an aircraft structure is optimized to minimize its weight. This means that certain areas of the fuselage skin and wing webs are allowed to undergo a state of elastic buckling, where visible folds that develop in the material leave no permanent deformations in the over-all structure when the loads are removed (Fig. 2). While in this buckled state, the aircraft skin is still capable of carrying load through tension-loaded bands of material located between the buckles. This condition is referred to as a state of diagonal tension.

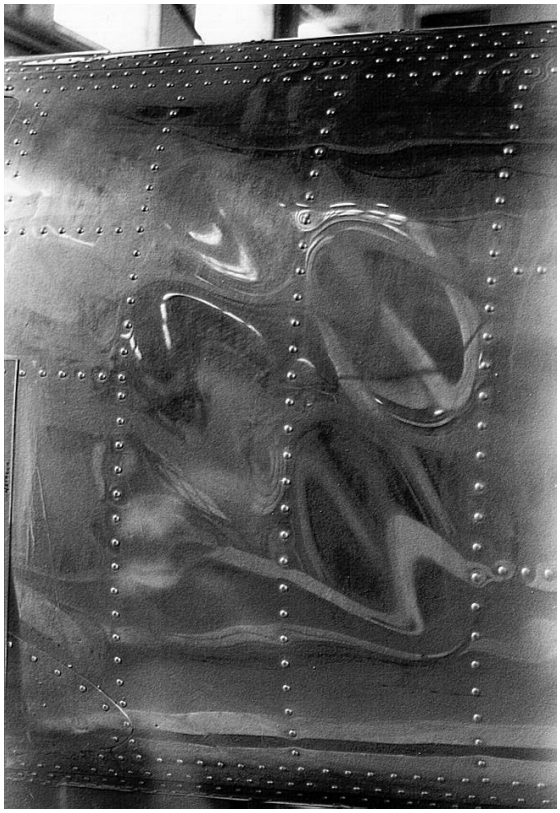

Fig. 2. Diagonal tension in a Canadair CT-114 Tutor

2 Diagonal Tension Theory

The following sections summarize the evolution of the NACA methodology for the diagonal tension phenomenon. A brief description of the original Wagner and Kuhn theories is given, followed by a history of additions and enhancements leading to the currently used semi-empirical methodology.

2.1 Wagner Theory (1929)

In 1929, German Professor Herbert Wagner realized that the aircraft design methods of the time were too conservative, and introduced the concept of diagonal tension, a theory he developed while working for the Rohrbach Metal Airplane Company [2, 3, 4]. Using conventional solid mechanics analysis he showed that, as a shear load is applied to a structure, the buckling only removes the compressive load carrying capacity of the web material. Wagner's original proof for his theory was convoluted, however, later publications provided a clearer description of Wagner's ideas [5, 6, 7, 8].

The basic principles of Wagner's theory state, that under a shear load a single web bay would react no differently than a simplified truss structure as shown in Fig. 3a, with two diagonal struts *A* and *B*. After applying a load ***P*** to the structure, strut *A* is loaded in tension while strut *B* has buckled and failed under the compressive load (Fig. 3b). Applying this concept to the stresses in a web panel, gives a uniform tension field working in a diagonal direction, without any compressive stresses (Fig. 3c).

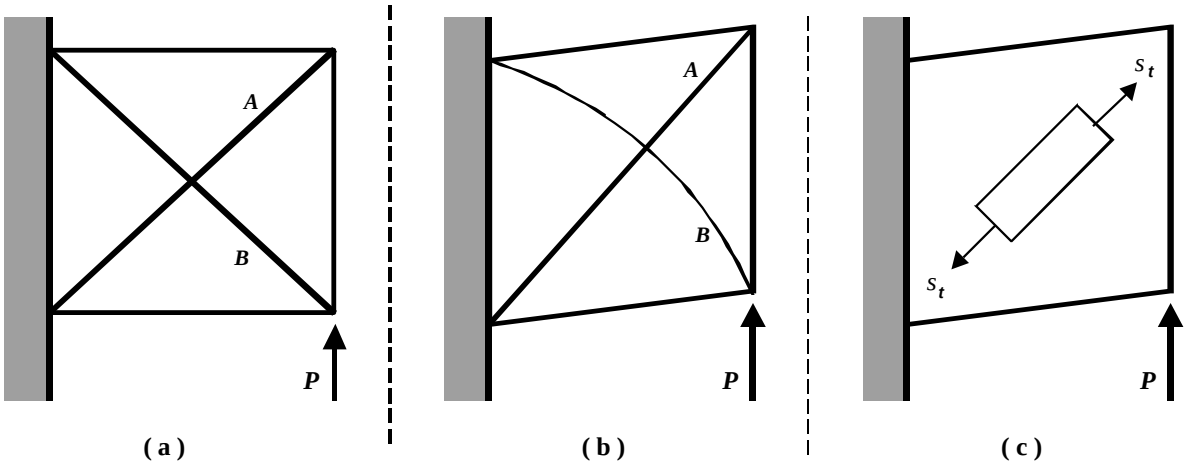

Fig. 3. Wagner principle of diagonal tension

2.2 NACA Theory (Paul Kuhn, 1952)

Paul Kuhn, a researcher at NACA, followed the theories developed by Wagner, and began more extensive studies into diagonal tension during the early 1930's. By the early 1940's, Kuhn had determined that Wagner's methods produced conservative results when used in the design of aircraft structures. He found that the buckled web of an aircraft beam was still capable of carrying compressive loads, due to a combination of pure shear (PS) and diagonal tension (DT) effects. This combined effect was called incomplete diagonal tension (IDT), as shown in Fig. 4.

Kuhn also found that the pure shear contribution to the stresses diminished as the shear load was increased. This balance between pure shear and diagonal tension components is referred to as the diagonal tension factor, and is typically denoted as ***k*** in the equations. When ***k*** is equal to 0, the web panel is unbuckled and under a state of pure shear. When ***k*** is between 0 and 1, the diagonal tension effect is increasing until a complete state of diagonal tension is reached (***k*** is equal to 1), as shown in Fig. 5.

These developments prompted another decade of work to analyze and confirm this theory. Kuhn summarized this body of work by May 1952, describing the basic theory [9] and the experimental evidence used to support his theories [10].

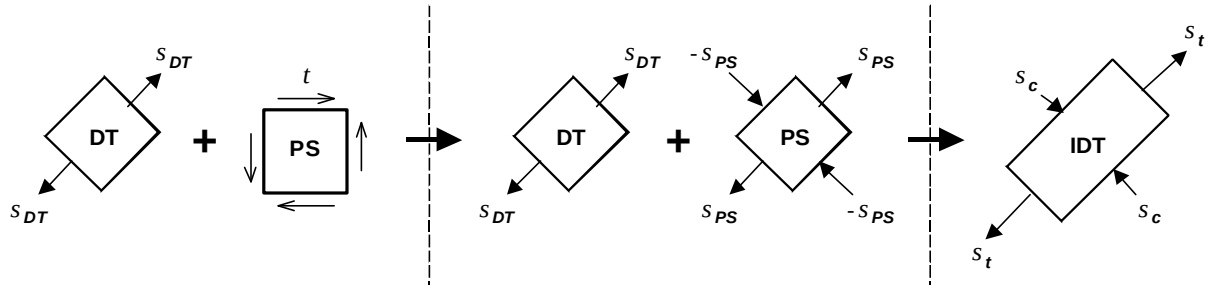

Fig. 4. NACA principle of diagonal tension

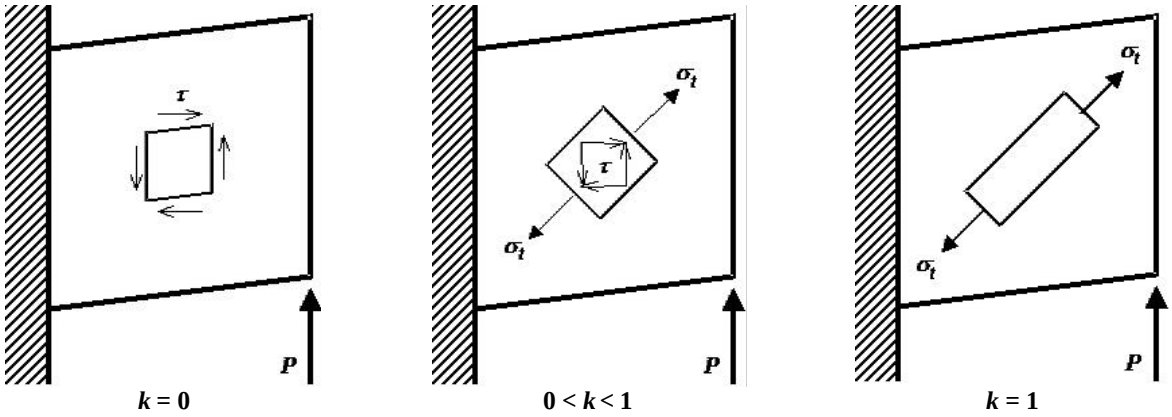

Fig. 5. NACA diagonal tension factor

2.3 Post-NACA Developments

Since the NACA research, several more attempts have been made to analyze the diagonal tension phenomenon. Some follow the NACA methodology while others developed alternate approaches.

2.3.1 The Grumman Modifications (1968)

Robert T. Ratay, of Grumman Aircraft Engineering Corporation, released a technical memorandum [11] listing modifications to the diagonal tension theory. This modification represented the beginning of a limited attempt to streamline and extend Kuhn's methodology to handle other materials and constructions not considered or tested by NACA. Key to this was the development of chemical milling, a technique, which had been used extensively to reduce the weight of the Orbiting Astronomical Observatory (OAO) and the Lunar Module (LM) spacecraft. For the type of test specimens being used [12], Grumman determined that the NACA method was typically conservative by 16% for web failures, and 13% for localized stiffener failures. However, it did correctly determine if either a web or a stiffener failure would occur. Determining column failure of the stiffeners was still considered too conservative, but no attempt was made to modify this prediction method. Ratay concluded that the NACA method, with modifications, was adequate for determining the ultimate load capacity of a stiffened beam design, with an acceptable conservatism.

2.3.2 The Boeing SST Developments (1970)

Research was started in the early-1970's to refine the theory for the design of the titanium structures used throughout the Boeing Super-Sonic Transport (SST) project [13, 14, 15]. The primary reasons were to meet the strict performance and economic requirements, which demanded a high level of structural efficiency. New allowables for titanium were required.

This study was conducted to take advantage of titanium's greater strength-to-weight advantage, as compared to an aluminum-based structure, and to develop the material allowables for use in the NACA methodology. However, titanium also seemed to exhibit other characteristics not evident in other materials: highly anisotropic properties, variations in the elastic modulus as a function of stress level, and a low shear-to-axial strength ratio. Most of the Boeing SST developments were in adjusting a design solution directly into a semi-empirical computer program. However, some of the published data was helpful in showing additions and modifications to the original NACA methodology.

2.3.3 Northrop Corporation (1985)

In 1985, Northrop Corporation, Aircraft Division released a report that includes modifications for using the Modified NACA methodology for anisotropic materials, such as aircraft composites [16]. Although intended for use in designing curved sections, key equations can be adjusted for use in designing

flat stiffened beams. However, none of the calculations for determining the diagonal tension effects were modified to account for anisotropic properties.

2.3.4 Structural Laminates Company (1997)

In early 1997, the Structural Laminates Company (SLC) outlined equations for calculating the stability of GLARE structures [17]. Included was a general theoretical overview for determining diagonal tension in GLARE. However, these corrections only affected the initial buckling calculation, and had not been experimentally proven. By 2000, an attempt was made to investigate the applicability of the modified NACA methodology for use in stiffened GLARE shear beams [18]. Two test panels were constructed using GLARE 3 – 5/4 and GLARE 4 – 5/4 skins, and were tested using the picture frame method. Predictions were made with hand calculations and finite element analysis. Unfortunately, the test panels proved to be too thick for the application of the NACA methodology. Therefore, it was not possible to study the post-buckling behaviour of GLARE. However, the project did validate the applied finite element methods. During the same year, plasticity effects of GLARE panels loaded in pure shear were also studied, but only for the simply supported boundary condition [19].

In all of these studies, it was found that GLARE could be treated as an isotropic material for most cases, up to the proportionality limit of the material. However, once the material entered a fully plastic state, the direction of the principal stresses has a large impact on the carrying capacity of the material due to the orthotropic load transfer into the glass fibres. Despite these studies, a need still existed to investigate the post-buckling behaviour of GLARE in a built-up structure.

3 NRC General Test Set-up

It was decided, that the specimen design would emulate the NACA diagonal tension tests [9, 10], and use the web dimensioning of NACA's Type I-25, small-size Wagner-beam test specimens (2.08 m x 0.66 m) shown in Fig. 6.

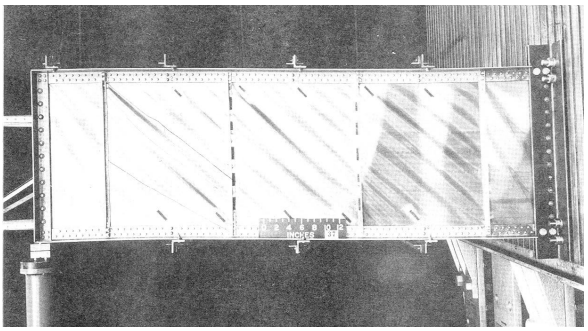

Fig. 6. NACA Type I-25 test specimen [10]

The replication of the stiffened beam design used by NACA was complicated because the original NACA engineering drawings were not available. Therefore, the NRC stiffened beam design, shown in Fig. 7, was developed through examination of the photos provided in the NACA technical notes, and by referring to basic aircraft and load frame design practices.

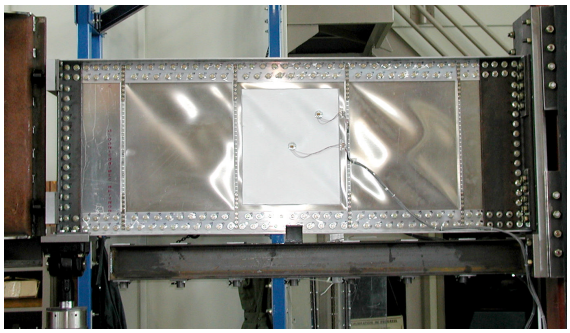

Fig. 7. NRC test specimen

All tests for this project were conducted using the Multi-Actuating Test (MAT) Platform, a new large-scale test facility developed by NRC-IAR-SMPL. This test structure is a large self-reacting steel space frame with the capacity to include additional structures, mounts, hard-points, and reinforcements to accommodate any tests that can be arranged within its boundaries. The stiffened FML flat beams were the first to use this new facility, and occupying the greater portion of one face of the platform (Fig. 8).

Additional columns and bracing were required to stiffen the platform for the purposes of the experiment. Plexiglas and Lexan shields were placed to protect personnel and equipment from flying debris, in the event of a catastrophic failure.

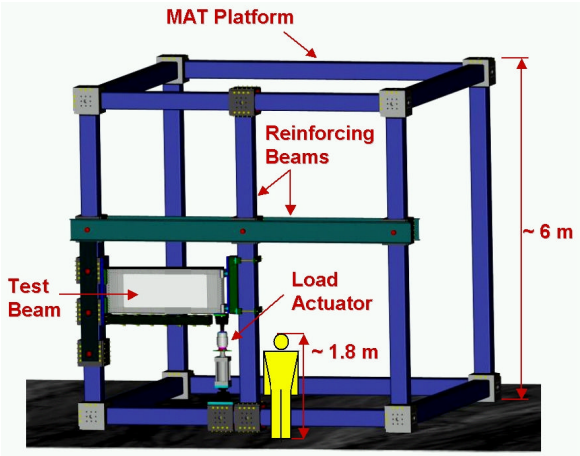

Fig. 8. Image of the MAT Platform

The test beams were attached through the support flanges to an interface plate, which was fixed to four clamp-on loading blocks (Fig. 9). The blocks were attached to a structural member of the MAT Platform, which was reinforced to provide extra stiffness and strength to the test frame. An additional structural member was secured ahead of the test specimen to provide more stiffness to the test frame as well as to provide a mount for the specimen anti-twist system.

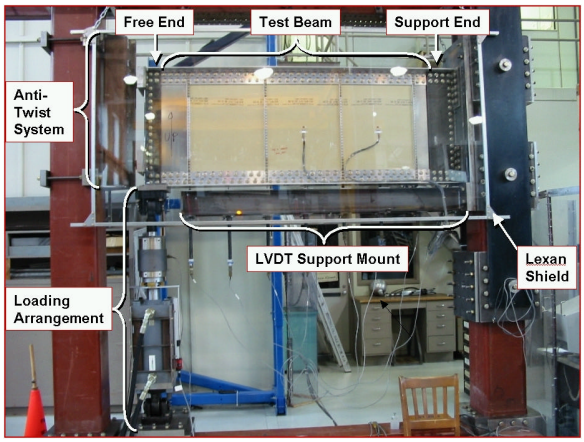

Fig. 9. General test set-up

4. Observations (Tests #1 to #4)

Four specimens were tested during the summer of 2001. However, the results were plagued with the premature failure of the flanges before the predicted critical failure of the web material. It soon became evident that efforts were needed to better understand the Diagonal Tension phenomenon by re-analyzing the prediction equations and understanding the test data.

4.1 Test #1: 1.27 mm 2024-T3 Aluminum

Test #1 was an aluminum baseline specimen to confirm the validity of the NACA methodology. During testing, it was noticed that from approximately 44.5 kN of applied load onward, the diagonal tension buckles in the web were clearly visible to the naked eye (Fig. 10).

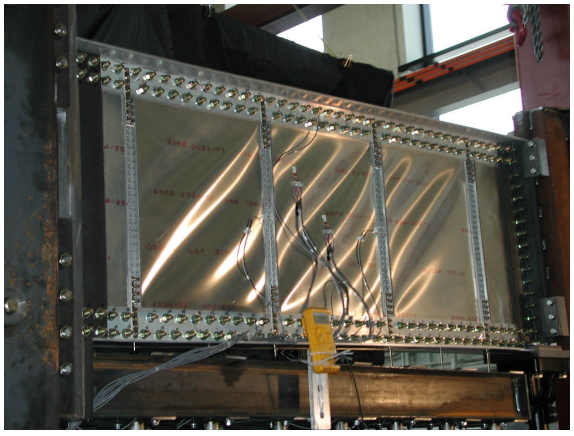

Fig. 10. Test Beam #1 at ~178 kN applied load

However, at an applied load of approximately 111 kN it was noticed that the test beam was absorbing load at a much slower rate than expected. At approximately 156 kN, strain readings from the central bay web did not appear to be high enough to lead towards a web failure. Deflection readings from the actuator LVDT were also much higher than expected, as discobration and a noticeable deflection difference was observed on the flanges near the support end of the beam. A decision was made to stop the test at an applied load of approximately 178 kN due to concerns that the flanges were yielding and that the web was no longer carrying sufficient load to induce a

critical web failure. After processing the data, it was found that the web had started to yield at ~111.7 kN at approximately 3100 µstrain. The maximum tensile strain reached in the web was 11,639 µstrain, at an applied load of 177.72 kN.

4.2 Test #2: GLARE 3– 3/2

Despite the results of the first test, it was decided to proceed with testing of the GLARE beams. As the applied load of 133 kN, was exceeded, the flanges began to exhibit deformation and discoloration similar to what was observed in Test #1. At an applied load of 226.39 kN and a tensile web strain of 45,193 µstrain, a combined failure of web and flanges was achieved (Fig. 11). After processing the data, it was found that the web had started to yield at ~88.7 kN at a strain of ~3100 µstrain.

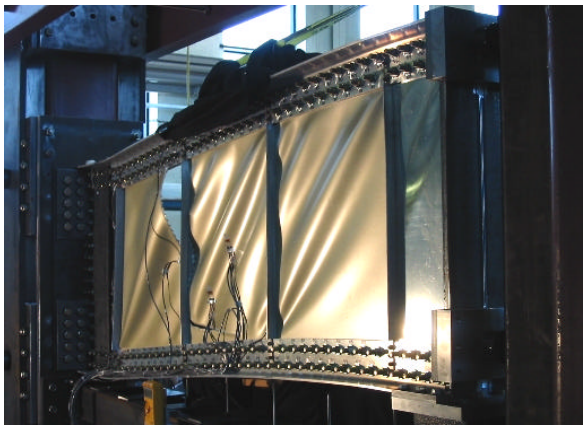

Fig. 11. Failure of Test Beam #2 after ~227 kN

Although the web clearly failed along the rivet and bolting lines, a closer examination of the failed flanges revealed large cracks in the vertical legs of the flanges, as seen in Fig. 12. These cracks followed one set of boltholes in the flanges, used for the stiffener's connection to the flange. In the opposite corners to the cracks, the flanges had locally buckled leaving a single large out-of-plane bulge in the vertical leg. This bulge was centred over the boltholes for the stringer/flange connection.

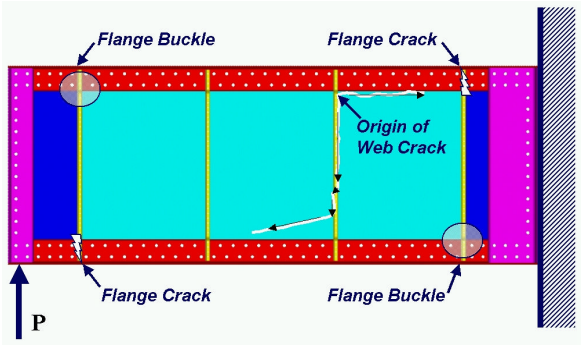

Fig. 12. Test #2 web and flange failures

4.3 Test #3: GLARE 3– 3/2

Beam #3 appeared to behave similar to Beam #2. As 133 kN was exceeded, the flanges again began to exhibit deformation and discoloration. The flanges suddenly failed at an applied load of 213.25 kN. After processing the data, it was found that the web had started to yield at ~88.8 kN at a strain of ~3100 µstrain. Unfortunately it was also found that the rosettes had started disbonding from the web between 178 kN and 200 kN, so no usable web strain data was recorded at the moment of beam failure.

4.4 Test #4: GLARE 4– 3/2

The GLARE 4-3/2 test provided similar reactions to the previous two tests. As the applied load of 156 kN, was exceeded, the flanges began to exhibit deformation and discoloration similar to what was observed in all previous tests. The flanges of test beam failed at an applied load of 228.05 kN, at a tensile web strain of 32,511 µstrain. Unfortunately, it was later discovered that the GLARE 4 – 3/2 sheet had been constructed incorrectly due to a manufacturing error.

5. The Elastic Strain Survey (Test #5)

A decision was made to address the concerns of possible distortions in the beam deflection readings and to better understand the unexpected flange failures. This was achieved by having the 1.80 mm 2024-T3 aluminum beam fitted with additional strain gauges and through reconfiguration of the LVDT placements. This extra instrumentation

allowed for a more detailed analysis of the diagonal tension phenomenon within the elastic limits of the beam design.

This test loaded the 1.80 mm 2024-T3 aluminum beam several times within the elastic limits to produce a strain survey of the structure. This data was used to calibrate the NRC and Bombardier FEA models, and the NACA methodology hand-calculations, within the elastic range. The data were combined with collected 1.27 mm and 1.80 mm aluminum stress-strain tensile test data to fine-tune the predictive methods. To meet this objective, forty strain gauge signals were added to the general set-up. The additional signals (mostly in the form of rosettes) were positioned to provide a strain survey of the central bay and to present a cross-section of the shear flow through the beam. An extra LVDT supporting structure was added to determine if there was any rotation between the beam and LVDT support mount interface locations on the MAT Platform.

6. Discussion

With insights from the Elastic Strain Survey and data from Test #1 through Test #4 were re-analyzed. Web data for the 1.27 mm 2024-T3 aluminum test beam (Fig. 13) shows a good comparison with the predicted results, even partially into the plastic region of web material. In the plastic range, there is a deviation due to the plasticity corrections used by NACA.

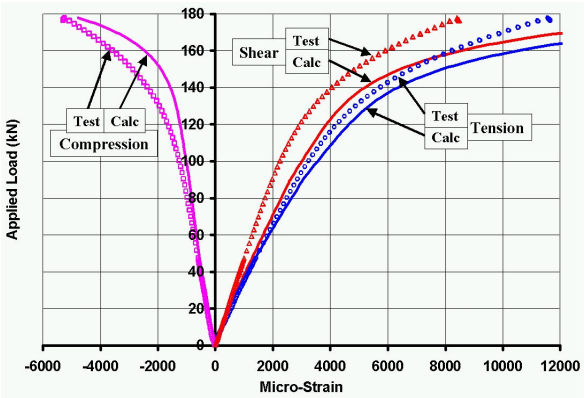

Fig. 13. Test #1 principal strains

The predictions for GLARE are only valid up to the yield point since GLARE has a different plastic behaviour than aluminum (Fig. 14). The 24S-T (2024-T3) aluminum plastic correction data were used for the GLARE predictions because no comparable data exists for GLARE at this time.

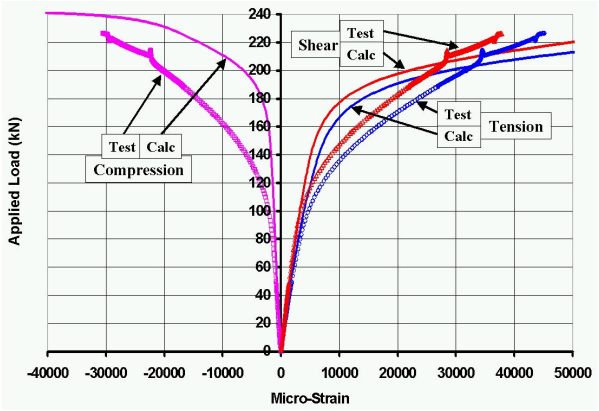

Fig. 14. Test #2 principal strains

Table 1, 2, and 3 show compare events within the elastic limits for each of the first four tests. Most predictions are within approximately 10% of the test values. This gives some evidence that the modified NACA methodology can be used for predicting GLARE behaviour below its yield point, as proposed by Grumman. Some of the deviation may be due to the loose-fit bolted construction of the flanges, balanced by the inherent 13% to 16% conservatism of the prediction equations. By contrast, Table 4 shows large differences in the mode and load values for the failure of the test beams. The failure of the compressive and tensile flanges seems to preempt any other failure modes.

Table 1: Revised Initial Buckling Comparison

Test #	Web Material	Thickness [mm]	Predicted [kN]	Test [kN]	Difference [%]
1	2024-T3 Al	1.27	5.60	5.30	-5.41
2	GLARE 3 – 3/2	1.42	6.22	7.55	21.39
3	GLARE 3 – 3/2	1.42	6.22	6.36	2.24
4	GLARE 4 – 3/2	1.68	8.59	9.21	7.24

Table 2: Web Shear Yielding Comparison

Test #	Web Material	Thickness [mm]	Predicted g [mstrain]	Predicted [kN]	Test [kN]	Difference [%]
1	2024-T3 Al	1.27	3071	101.63	123.21	21.23
2	GLARE 3 – 3/2	1.42	1836	61.24	65.30	6.63
3	GLARE 3 – 3/2	1.42	1836	61.24	65.31	6.66
4	GLARE 4 – 3/2	1.68	1598	59.72	60.21	0.83

Table 3: Web Tensile Yielding Comparison

Test #	Web Material	Thickness [mm]	Predicted e [mstrain]	Predicted [kN]	Test [kN]	Difference [%]
1	2024-T3 Al	1.27	3772	104.23	111.65	7.13
2	GLARE 3 – 3/2	1.42	3853	98.52	88.66	-10.01
3	GLARE 3 – 3/2	1.42	3853	98.52	88.80	-9.86
4	GLARE 4 – 3/2	1.68	4137	103.89	95.68	-7.90

Table 4: Revised Web Failure Comparison

Test #	Web Material	Thickness [mm]	Predict Web Fail [kN]	Test [kN]	Failure Mode	Difference [%]
1	2024-T3 Al	1.27	167.53	177.72	N / A	6.08
2	GLARE 3 – 3/2	1.42	189.83	226.39	Web/Flng	19.26
3	GLARE 3 – 3/2	1.42	189.83	213.25	Flange	12.34
4	GLARE 4 – 3/2	1.68	223.39	229.38	Flange	2.09

Therefore, the modified NACA method cannot accurately predict the final failure of the NRC test beams. Unfortunately, no solution or prediction method has been found to account for the stress concentrations forming at the corners of the beam test section. This leads to two possible arguments: either the modified NACA method is still too conservative for estimating the web stress/strain reactions, or more effort is required to improve the corrections that describe the plastic behaviour of aluminum and GLARE. Thus, under its current configuration, the NRC test beam will not produce a web specific failure in the remaining test specimens. It is expected that specimen flanges will yield and locally fail before sufficient strain can be developed to fracture the web.

7. Conclusions

A large amount of useful information was collected in this work, and this resulted in a better understanding of the diagonal tension phenomenon. The review of the diagonal tension methodology resulted in a better understanding of the NACA theory and corrections to certain predictions. By using the existing hand-calculation methods within the elastic range of the beam design, it is possible to estimate the diagonal tension reaction of GLARE beams. The modified NACA methodology has been shown to provide

excellent predictions for the GLARE and aluminum specimens, up to the Grumman criterion for determining the yielding of the web material. It was also found that the historical empirical data used for determining the plasticity effects in 2024-T3 aluminum needs to be revised. However, more data needs to be collected to properly predict GLARE's reaction within the plastic range and to estimate the allowables for a web failure. This has led to some differences of opinion regarding the mode of failure to be used in the design of GLARE structures, between the yielding criteria presented by Grumman and the failure criteria presented by NACA.

References

[1] Asundi, A.; Choi, Alta Y. N.; ***Fiber Metal Laminates: An Advanced Material for Future Aircraft***; Journal of Materials Processing Technology, Vol. 63, No. 1, pg 384-394: January 1997.

[2] Wagner, Herbert; ***Flat Sheet Metal Girders with Very Thin Metal Web, Part I – General Theories and Assumptions***; NACA-TM-604; Washington: February 1931.

[3] Wagner, Herbert; ***Flat Sheet Metal Girders with Very Thin Metal Web, Part II – Sheet Metal Girders with Spars Resistant to Bending, Oblique Uprights – Stiffness***; NACA-TM-605; Washington: February 1931.

[4] Wagner, Herbert; ***Flat Sheet Metal Girders with Very Thin Metal Web, Part III – Sheet Metal Girders with Spars Resistant to Bending, The Stress in Uprights – Diagonal Tension Fields***; NACA-TM-606; Washington: February 1931.

[5] Kuhn, Paul; ***A Summary of Design Formulas for Beams Having Thin Webs in Diagonal Tension***; NACA-TN-469; Washington: August 1933.

[6] Peery, David J.; Azar, Jamal J.; ***Aircraft Structures***; 2nd edition; McGraw-Hill: 1982.

[7] Bruhn, E. F.; ***Analysis and Design of Flight Structures***; Tri-State Offset: 1973.

[8] Megson, T. H. G.; ***Aircraft Structures for Engineering Students***; 3rd edition; Arnold Publishers: 1999.

[9] Kuhn, Paul; Peterson, James P.; Levin, L. Ross; ***A Summary of Diagonal Tension, Part I – Methods of Analysis***; NACA-TN-2661; Langley Field: May 1952.

[10] Kuhn, Paul; Peterson, James P.; Levin, L. Ross; ***A Summary of Diagonal Tension, Part II – Experimental Evidence***; NACA-TN-2662; Langley Field: May 1952.

[11] Ratay, Robert T.; ***Instability and Failure Analysis of Flat Stiffened Plates Under Shear (Modified NACA Method)***; Structural Mechanics Note No.14; Grumman Aircraft Engineering Corporation: November 1968.

[12] Tsongas, Alexander G.; Ratay, Robert T.; ***Investigation of Diagonal-Tension Beams with Very Thin Stiffened Webs***; Contract NAS 9-8284; Grumman Aerospace Corporation: July 1969.

[13] Musgrove, Max D.; Mortensen, Robert E.; ***Development of Titanium Structural Element Allowables for the Boeing SST***; AIAA/ASME 11th Structures, Stuctural Dynamics and Materials Conference: April 1970.

[14] Mello, Raymond M.; Sherrer, Robert E.; Musgrove, Max D.; ***Intermediate Diagonal Tension Filed Shear Beam Development for the Boeing SST***; AIAA/ASME 12th Structures, Stuctural Dynamics and Materials Conference, (Anaheim, California / April 19-21, 1971), Paper No. 71-340: April 1971.

[15] Barevics, Vilis M.; Hoy, J. Douglas; Sherrer, Robert E.; ***SST Technology Follow-On Program - Phase I, Intermediate Shear Beam Analyses***; Boeing Company Report No. FAA-SS-72-11; Seattle: May 1972.

[16] Deo, R. B.; Agarwal, B. L.; Madenci, E.; ***Design Methodology and Life Analysis of Postbuckled Metal and Composite Panels***; Northrop Corporation, Aircraft Division Report AFWAL-TR-85-3096, Vol. 1; Hawthorne: December 1985.

[17] van Wimersma, B.; van Oost, R. C.; Roebroeks, G.; Gunnick, J. W.; ***Stability of GLARE Structures - Calculation Method***; Structural Laminates Company, Report: TD-R-97-001: February 1997.

[18] Wittenberg, T. C.; de Boer, A.; ***Design of FML Shear Panels for Ultra-High Capacity Aircraft***; Delft University of Technology: 2000.

[19] Wittenberg, T. C.; van Baten, T. J.; ***Plastic Buckling Analysis of Flat Rectangular FML Plates Loaded in Shear***; Advanced Materials and Processes: Technology and Economics, Proceedings of the 32nd International SAMPE Technical Conference, Boston, Nov 5-9, 2000, pg 673-686: November 2000.